Engineering Perspective 4 (2): 60-68, 2024

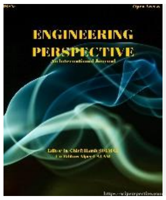

e-ISSN:2757-9077

ENGINEERING PERSPECTIVE

https://sciperspective.com/

Research Paper

Modeling and Simulation of Integrated Photovoltaic-Alkaline Electrolyzer System for Sustainable Hydrogen Production

Fatima Haidar [1*], Imen Mrad [1], Quang Truc Dam [1]

[1] *Capgemini Engineering, Research & Innovation Direction, 12 rue de la Verrerie, 92190, Meudon, France*

ABSTRACT

In this research, the integration of an alkaline electrolyzer system with a photovoltaic (PV) array is explored to facilitate the green production of hydrogen. By directly coupling these two technologies, solar energy is harnessed to drive the electrolysis process, consequently generating hydrogen as a sustainable energy carrier. To enable accurate simulation and analysis of the integrated system, a novel methodology is introduced for identifying and quantifying the various parameters crucial for understanding the electrical behavior of the alkaline electrolyzer system. Through this method, the interplay between the PV array's output and the electrolyzer's operation can be comprehensively captured, allowing for precise modeling of the overall system dynamics. Moreover, mathematical equations are established to provide insights into the anticipated quantities of hydrogen generated by the electrolyzer system under different operating conditions. These equations serve as predictive tools, offering valuable insights into the system's performance and efficiency, essential for optimizing its design and operation. The proposed methodology and equations are implemented and validated using the MATLAB/Simulink environment, a powerful tool for simulating complex systems. By leveraging this platform, the integrated PV-electrolyzer system can be simulated with high fidelity, capturing its dynamic behavior and performance characteristics under varying scenarios. The promotion of renewable energy-based solutions for sustainable hydrogen production is aimed to be facilitated by this research, thereby contributing to the transition towards a greener and more resilient energy future.

Keywords: Alkaline Electrolyzer; Hydrogen; Mathematical Modeling; Solar System.

History
Received: 15.01.2024
Accepted: 03.05.2024

Author Contacts
**Corresponding Author*
e-mail addresses: Fatima.haidar@capgemini.com, Imenmrading@gmail.com, Quang-truc.dam@capgemini.com

How to cite this paper:
Haidar, F., Mrad, I., Dam, Q.T., (2024). Modeling and Simulation of Integrated Photovoltaic-Alkaline Electrolyzer System for Sustainable Hydrogen Production. Engineering Perspective, 4 (2), 60-68. http://dx.doi.org/10.29228/eng.pers.76380

1. Introduction

The global energy landscape is undergoing a profound transformation driven by the increasing demand for energy and the imperative to mitigate the impacts of climate change [1 - 2]. As traditional fossil fuel reserves dwindle and concerns over greenhouse gas emissions escalate, there is an urgent need to explore and develop new sources of clean and sustainable energy [3]. Renewable energy sources, such as solar and wind power, have emerged as pivotal components of the transition towards a more environmentally friendly energy paradigm [4]. However, despite their abundance and potential, the widespread adoption of renewable energy faces significant challenges, including intermittency and the efficient storage and conversion of energy into electricity [5]. One of the key challenges in harnessing renewable energy is the intermittent nature of sources such as solar and wind power. Unlike conventional fossil fuels, which provide a continuous and reliable source of energy, renewable sources fluctuate with weather conditions and time of day, presenting operational difficulties for their integration into existing electrical grids [6]. To address this challenge, there is a pressing need for innovative energy storage solutions that can store excess energy during periods of abundance and release it when needed [7]. In recent years, electrochemical storage systems, such as batteries and hydrogen fuel cells, have garnered significant attention as potential solutions to the energy storage problem [8]. Hydrogen, in particular, has emerged as a versatile energy carrier with the potential to store and transport energy derived from renewable sources [9]. The electrochemical conversion of hydrogen in fuel cells offers a clean and efficient way to generate electricity, with water vapor being the only byproduct [10]. However, the widespread adoption of hydrogen as an energy carrier is hindered by challenges related to its production, storage, and distribution [6].

While most of today's hydrogen production methods rely on fossil fuels, there is growing interest in developing technologies that can directly convert renewable energy, such as solar power, into hydrogen [7], [11]. Among these technologies, the coupling of solar panels with electrolyzers has emerged as a promising approach for green hydrogen production [5]. By leveraging solar energy to power the electrolysis of water, this technique offers a sustainable and carbon-neutral method for producing hydrogen [12]. The efficiency of this process can reach up to 13%, making it a viable option for large-scale hydrogen production [8].

Electrolyzers, the key components in this process, come in several different technologies, including alkaline, membrane, and high-temperature steam electrolyzers [13]. Using those technologies, water is dissociated into hydrogen and oxygen gases through the application of an electric current. Of these, alkaline electrolyzers are one of the most established and widely used technologies for hydrogen production. They operate by utilizing an alkaline electrolyte, typically potassium hydroxide (KOH) or sodium hydroxide (NaOH), and electrodes made of materials like nickel or stainless steel. Alkaline electrolyzers offer several advantages, including relatively low capital costs, high efficiency, and long operational lifetimes. They are suitable for large-scale hydrogen production applications, such as industrial hydrogen generation, renewable energy storage, and transportation fuel production. Additionally, alkaline electrolyzers can operate at ambient temperatures and pressures, simplifying their integration into existing industrial processes and infrastructure. These attributes make Alkaline electrolyzers well-suited for integration with renewable energy sources, such as solar power [3], [9], [11].

In this study, the focus lies on the modeling and simulation of a photovoltaic system integrated with an alkaline electrolyzer for hydrogen production via water electrolysis. The electrolysis process is driven by the electrical energy provided by photovoltaic panels, with excess energy being stored in the form of hydrogen [14 - 16]. Utilizing advanced modeling techniques and simulation tools like MATLAB/Simulink, emphasis is placed on optimizing the performance of the integrated system and identifying the most favorable conditions for efficient hydrogen production. Through this research, a contribution is aimed to be made towards the advancement of sustainable energy solutions and the acceleration of the transition towards a greener and more resilient energy future.

The flowchart as shown in Figure 1 outlines the study's progression, beginning with an introduction to global energy challenges and the significance of transitioning to renewable energy sources, particularly hydrogen. Motivation is provided for exploring sustainable hydrogen production methods, leading to the integration of photovoltaic and electrolyzer systems for green hydrogen generation. In *section 2*, theoretical principles of hydrogen production and design concepts for photovoltaic and alkaline electrolyzer systems are then elucidated. Mathematical modeling follows, detailing the development of equations to describe PV panel and electrolyzer behaviour, including factors influencing hydrogen production rates. *Section 3* is devoted to simulation setup for implementing these models using

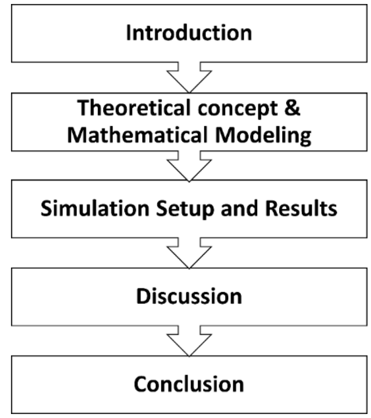

Figure 1. Flowchart summarizing the entire study.

MATLAB/Simulink and configuring the integrated PV-electrolyzer system and its result. Discussion analysis entails examining simulation data on PV module performance and hydrogen production rates, elucidating trends and correlations between variables is presented in *section 4*. Finally, the conclusion summarizes findings regarding system performance and efficiency, while also suggesting future research directions for energy storage and grid integration solutions.

2.2. Theoretical concept of alkaline Technology and PV system

2.2.1. Principle of hydrogen production

The principle of hydrogen production [13] within the system under study encompasses three primary subsystems, each integral to the overall process:

Firstly, the production of renewable electric energy serves as the initial step in the hydrogen production chain. This process relies heavily on the utilization of photovoltaic panels, converting incident solar radiation into electricity through the photovoltaic effect. The electricity generated by the solar panels serves as the primary energy source for the subsequent electrolysis of water, thus initiating the production of hydrogen [13]. Secondly, the electrolysis of water represents the pivotal stage wherein water molecules are dissociated into their constituent elements, hydrogen and oxygen. Various electrolysis techniques are employed for this purpose, with alkaline electrolyzers, polymer membrane electrolyzers, and ceramic oxide electrolyzers being the most commonly utilized methods. These electrolysis techniques facilitate the efficient separation of hydrogen and oxygen gases, enabling the selective extraction of hydrogen for subsequent storage and utilization.

Lastly, the storage of gases constitutes the final component of the hydrogen production process. This phase involves the collection and containment of the produced hydrogen gas for future use. Commonly employed techniques for hydrogen storage include liquefaction and hydration processes. Liquefaction involves cooling the hydrogen gas to extremely low temperatures, thereby converting it into a liquid state for denser and more compact storage. Alternatively, hydration methods involve the absorption of hydrogen gas into a solid matrix, such as metal hydrides, for safe and efficient storage [13], [17].

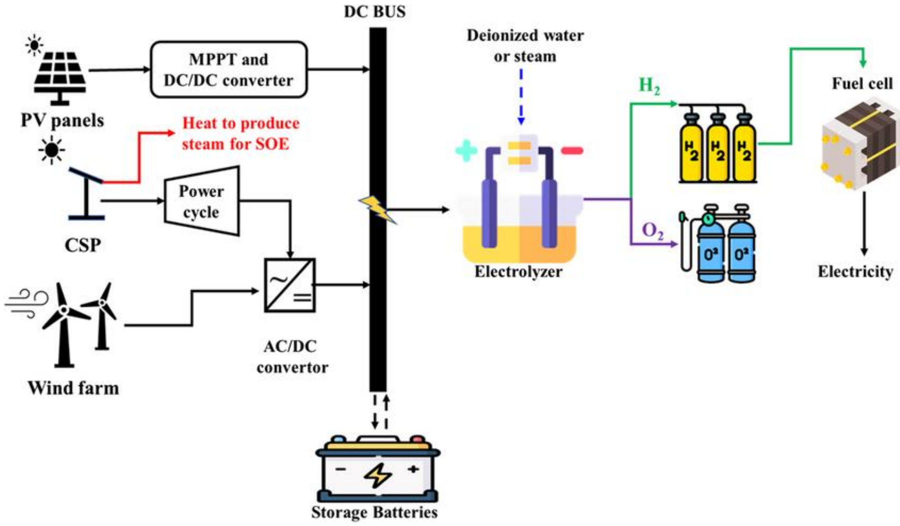

Figure 2. Configuration and operational principles of the Hydrogen production facility [13].

The configuration and operational principles of the hydrogen production facility are depicted in Figure 2, illustrating the interconnectedness of the various subsystems involved in the process. The efficient coordination and integration of these subsystems are essential for optimizing hydrogen production efficiency and ensuring the viability of the overall system. Through continuous research and development efforts, advancements in each of these subsystems contribute to the realization of sustainable and scalable hydrogen production solutions, thereby facilitating the transition towards a cleaner and more sustainable energy landscape.

2.2.2. Designing the Photovoltaic System

In the realm of renewable energy systems, the photovoltaic (PV) generator stands as a cornerstone for sustainable energy production [14 - 16]. In this study, the photovoltaic system's energy production is predominantly facilitated by the photovoltaic generator, which harnesses solar radiation to generate electricity. Leveraging the climate data specific to the site, including sunshine duration and ambient temperature, alongside module specifications provided by the manufacturer, enables precise estimation of the energy output achievable by the photovoltaic module.

The mathematical model of a photovoltaic generator relies on an equivalent circuit. In Figure 3 below, the equivalent circuit is depicted, featuring a current source I_{ph} representing the photocurrent generated by the cell, with R_s and R_{sh} denoting the inherent shunt and series resistances of the cell, respectively, along a diode in parallel [1-3].

PV cells are assembled into larger units known as PV modules, which are then interconnected in a parallel-series arrangement to create PV arrays. Typically, R_{sh} has a very high value, and R_s has a very low value, thus they can often be disregarded to simplify the analysis.

The mathematical model of the photovoltaic panel is described as following in the Eq. (1):

$$I_{ph} = \left[I_{sc\ ref} + Ki\ \left(T - T_{ref}\ \right)\right] \times Insol \tag{1}$$

Where, $I_{sc\ ref}$ is the short-circuit current (ISC) at reference temperature, Ki denotes the short-circuit current temperature co-efficient, T is the operating temperature of the module, T_{ref} is the reference temperature of the module, and $Insol$ is the Input current of a PV module.

The reverse saturation current (I_{rs}) is calculated as following in the Eq. (2):

$$I_{rs} = I_{sc}/[exp(\frac{qV_{oc}}{N_s kAT_{ref}} - 1] \tag{2}$$

Where N_s is the total number of cells in series, V_{oc} is the open circuit voltage, q represents the Electron charge, k denotes the Boltzmann constant, and A is an idealist factor.

The module's saturation current is then calculated using Eq. (3):

$$I_s = I_{rs}\left[\frac{T_a}{T_{ref}}\right] exp[\frac{q \times E_{g0}}{Bk}\ \left(\frac{1}{T_{ref}} - \frac{1}{T_a}\right)] \tag{3}$$

Where, E_{g0} is the band gap for silicon, $B = A$, and T_a is the operating temperature of the module.

Hence, the calculation of the photovoltaic panel current can be expressed as follows in the Eq. (4):

$$I_{PV} = N_p \times I_{ph} - N_p \times I_0 \left[exp\left(\frac{q \times V_{PV} + I_{PV}R_s}{N_s kAT}\right) - \ 1\right] \tag{4}$$

Where, N_p represents the number of cells connected in parallel, and V_{PV} is the output voltage of a PV module.

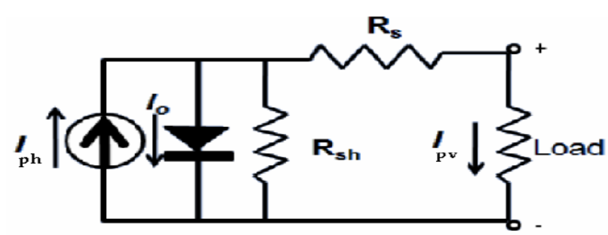

Figure 3. PV cell modelled as an equivalent circuit with diodes

2.3. Designing the Alkaline Electrolyzer System

An electrolyzer serves as a pivotal device in the production of hydrogen, leveraging electrical energy to facilitate the electrolysis of water into its constituent elements, hydrogen, and oxygen, via an electrochemical process. To facilitate the splitting of water molecules, a direct current (DC) must be applied across two electrodes immersed in an aqueous electrolyte with high ionic conductivity (Tijani et al., 2014; Ulleberg, 2003). Typically, the overarching reaction for water splitting is represented as follows in the Eq. (5):

$$H_2O_{(l)} + electrical\ \ energy \tag{5}$$

By using the stoichiometry, the production rate of water consumption and oxygen also can be determined as in the Eq. (6):

$$\dot{n}_{H_2O} \ = \dot{n}_{H_2,prod} \ = \ 2\dot{n}_{O_2} \tag{6}$$

In this study, emphasis is placed on the Alkaline electrolyzer, chosen for its efficiency in hydrogen production. The water electrolyzer comprises multiple electrolyzer cells interconnected either in series, parallel, or both. Our electrolyzer model is intricately designed based on the characteristics of individual cells, with parameters such as operating voltage and gas flow rates determined per cell. Scaling up to the entire electrolysis unit involves simple multiplication of these values by the number of cells in series and parallel. For the sake of modelling the electrolyzer, its mathematical model will be analysed in the following:

The thermal model uses current and voltage, to calculate the temperature variation within the electrolyzer cell by modeling the following equation Eq. (7):

$$C_t \frac{dT}{dt} = \ \dot{q}_{gen} - \dot{q}_{loss} - \dot{q}_{cooling} \tag{7}$$

Where, T is the Cell temperature in Kelvin, C_t denotes the Overall thermal capacity of the electrolyzer, $\dot{q}_{gen}$ is the Heat power generated inside the electrolyzer, $\dot{q}_{loss}$ is the Heat power loss and $\dot{q}_{cooling}$ is the Cooling heat power.

For reference (details provided below for each calculation):

→ $\dot{q}_{aen}$ → Can be written as: $\dot{q}_{gen} = \ (V - V_{th}) \times I$ with $V_{th} = \frac{-\Delta H}{2F}$

→ $\dot{q}_{loss}$ → Can be determined by: $\dot{q}_{loss} = \frac{1}{R_t} \ (T - T_{amb})$ with R_t is the thermal resistance of the electrolyzer and T_{amb} is the ambient temperature.

→ $\dot{q}_{cooling}$ → Can be expressed as $\dot{q}_{cooling} = C_m \times (T_{cm,s} - T_{cm,e})$ with C_m is the thermal capacity of the cooling water, $T_{cm,s}$ is the inlet cooling water temperature, and $T_{cm,e}$ is the outlet cooling water temperature with:

$$T_{cm,s} = \ T_{cm,e} + \left(T - T_{cm,e}\right) + (1 - \exp(-\frac{V_{AHX}}{C_m}))$$

and V_{AHX} is the overall heat transfer coefficient. It is obtained by the following equation: $V_{AHX} = h_{cond} + h_{conv}.I$ where, h_{cond} and h_{conv} are the parameters related respectively to heat transfer by conduction and by convection.

The overall energy balance is defined as in the Eq. (8):

$$\frac{dT}{dt} + aT - b = 0 \tag{8}$$

The solution to the differential equation of the balance is given by the Eq. (9):

$$T(t) = \ \left(T_{ini} - \frac{b}{a}\right) exp(-at) + \frac{b}{a} \tag{9}$$

With:

$$a = \ \frac{1}{R_t.C_t} + \frac{C_{cm}}{C_t}\left(1 - exp\left(-\frac{V_{AHX}}{C_{cm}}\right)\right)$$

$$b = \frac{n_c(V - V_{th}).I}{C_t} + \frac{T_{amb}}{R_t C_t} + \frac{C_{cm} T_{cm,c}}{C_t}\left(1 - exp\left(-\frac{V_{AHX}}{C_{cm}}\right)\right) \tag{10}$$

In a non-spontaneous electrochemical process, the change in free energy is equivalent to the electrical work required for the reaction to occur. The cell voltage U_{Ecell}, expressed in volts is defined by the Eq. (11):

$$U_{Ecell} = \ U_{rev} + \frac{r_1 + r_2 T}{A} I + s \ln\left(\frac{t_1 + \frac{t_2}{T} + \frac{t_3}{T^2}}{A} I + 1\right) \tag{11}$$

Where, r_1 and r_2 represent the parameters of ohmic resistance (Ω.m^2, Ω.m^2/°C), s is the Ohmic voltage (V), t_1, t_2 and t_3 are the overvoltage parameters; t_1 (m^2·A^{-1}), t_2 (m^2.C.A^{-1}), t_3 (m^2.C^2/A^{-1}), A is the area of the cell electrode (m^2), I represents the electrolyzer current in (A), T is the cell temperature (°C) and U_{rev} is the reversible voltage (V).

When assuming a reversible reaction, the energy of the process (H) is utilized with a reversible voltage as indicated in the following reaction (12):

$$U_{rev} = \frac{\Delta G}{ZF} \tag{12}$$

Where, ΔG represents the Gibbs free energy, Z is the number of electrons (2e$^-$), which is the number of molecules transferred per molecule of hydrogen, equal to 2, F is a Faraday's constant (96500 C), U_{rev} which can be expressed by an empirical equation as: $U_{rev} = U_{rev}^0 - k_{rev}(T - 25)$ where U_{rev}^0 denotes the reversible cell voltage under standard conditions and k_{rev} is the empirical temperature coefficient of U_{rev} (V/°C).

The cells of an electrolyzer are connected in series, so the current is the same and the voltage is given by the following Eq. (13):

$$U_E = n_C . U_{Ecell} \tag{13}$$

The amount of hydrogen generated can be calculated from the voltage and current of the electrolyzer as in the following Eq. (14):

$$\dot{n}_{H_2,prod} = \eta_F \frac{N_c I}{ZF} \tag{14}$$

Where Z is equal 2.

According to Faraday's law, the production of hydrogen is influenced by the rate of electron transfer at the electrodes, which corresponds to the electrical current in the external circuit. Conversely, Faraday efficiency represents the ratio of actual hydrogen production to the theoretical maximum achievable in the electrolyzer. However, Faraday efficiency can be compromised by parasitic current losses, which increase as current densities decrease due to higher electrolyte share, leading to reduced electrical resistance. Moreover, temperature elevation results in decreased resistance, amplifying parasitic current losses and consequently lowering Faraday efficiency which can be determined as in the following Eq. (15):

$$\eta_F = \frac{\left(\frac{I}{A}\right)^2}{f_1 + \left(\frac{I}{A}\right)^2} f_2 \tag{15}$$

Where, I is the current of the electrolyzer, n_C is the number of particles (21), A represent the Effective surface 0.25, f_1 and f_2 denotes the calculation parameters of the faradic efficiency 250 mA^2/cm^4, 0.96 respectively, $\dot{n}_{H_2,prod}$ is the rate of hydrogen production (mol/s) and η_F is the Faradaic efficiency.

The determination of the volume flow rate of hydrogen is influenced by several factors inherent to the electrolysis process and the operational parameters of the electrolyzer system. Key factors include the current density applied to the electrolyzer, the efficiency of the electrolysis process, the temperature and pressure conditions within the system, and the composition of the electrolyte used. Additionally, factors such as the electrode surface area and the design of the electrolyzer cells can also impact the volume flow rate of hydrogen. The hydrogen production rate, denoted by $\dot{n}_{H_2,prod}$, is initially measured in units of mol/s, representing the amount of hydrogen generated per unit time. To convert this rate into a more commonly used unit for industrial applications, such as Nm³/h (normal cubic meters per hour), a series of conversions are applied. Firstly, to convert from mol/s to mol/h, the production rate is multiplied by the number of seconds in an hour (3600), extending the measurement to an hourly basis. Subsequently, to account for the volumetric properties of gases under standard conditions (typically defined as 1 atm pressure and 0°C temperature), the production rate is multiplied by the molar volume of an ideal gas at these conditions. This value, commonly denoted by V_m is approximately 0.022414 m³/mol. Therefore, the equation for Q, representing the hydrogen production rate in Nm³/h, is derived as follows in Eq. (16):

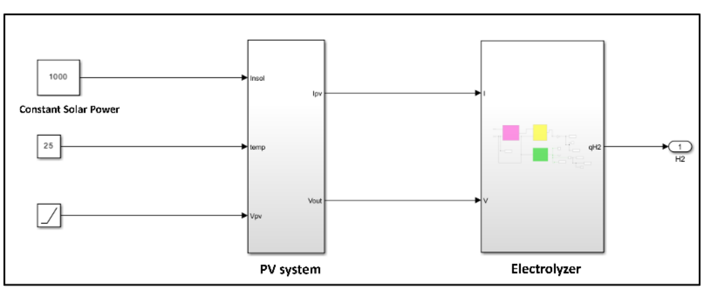

Figure 4. Simulation model of direct coupling of an electrolyzer to PV system

$$Q = \dot{n}_{H_2,prod} \times 3600 \times 0.022414 \tag{16}$$

3. Simulation results

The integration of an alkaline electrolyzer system with a photovoltaic (PV) array for green hydrogen production has been extensively explored in this research. Through simulation and analysis using MATLAB/Simulink environment, the dynamic behaviour and performance characteristics of the integrated PV-electrolyzer system have been investigated. This setup was established to illustrate the configuration depicted in Figure 4.

The simulation model, as depicted in Figures 4 integrates the PV system with the alkaline electrolyzer, allowing for the direct coupling of solar energy to drive the electrolysis process for hydrogen production.

The PV model comprises six interconnected subsystems as shown in Figure 5 and represent the calculation to modelized the PV using Eq. (1) to Eq. (4), while the electrolyzer model in Figure 6, consists of three sub-systems: thermal, electrochemical, and hydrogen production models. The Eq. (7) to (15) represent the calculation to modelized the alkaline Electrolyzer coupled to PV system.

- **PV with single cell ($N_p = 1$)**

Firstly, the performance of the PV module with a single cell ($N_p = 1$) was analysed under varying irradiation conditions at a constant temperature of 25 °C. Figures 7, 8, and 9 illustrate the I-V and P-V characteristics of the PV module, showing the module's current, voltage, and power output under different irradiation levels. The input irradiation is shown in Figure 7. Between 0 and 1 s, the irradiation is 200 W/m^2, between 1 and 2 s it is 600 W/m^2, while from 2 s onwards it is 1000 W/m^2.These results provide insights into the PV system's behaviour and performance under changing environmental conditions.

Figure 8 illustrates the relationship between module current I_{PV} and module voltage V_{PV} for varying levels of irradiation. Each curve represents a different irradiation level: 200 W/m^2, 600 W/m^2, and 1000 W/m^2. As expected, at higher irradiation levels, the module current is generally higher across the entire voltage range. This is

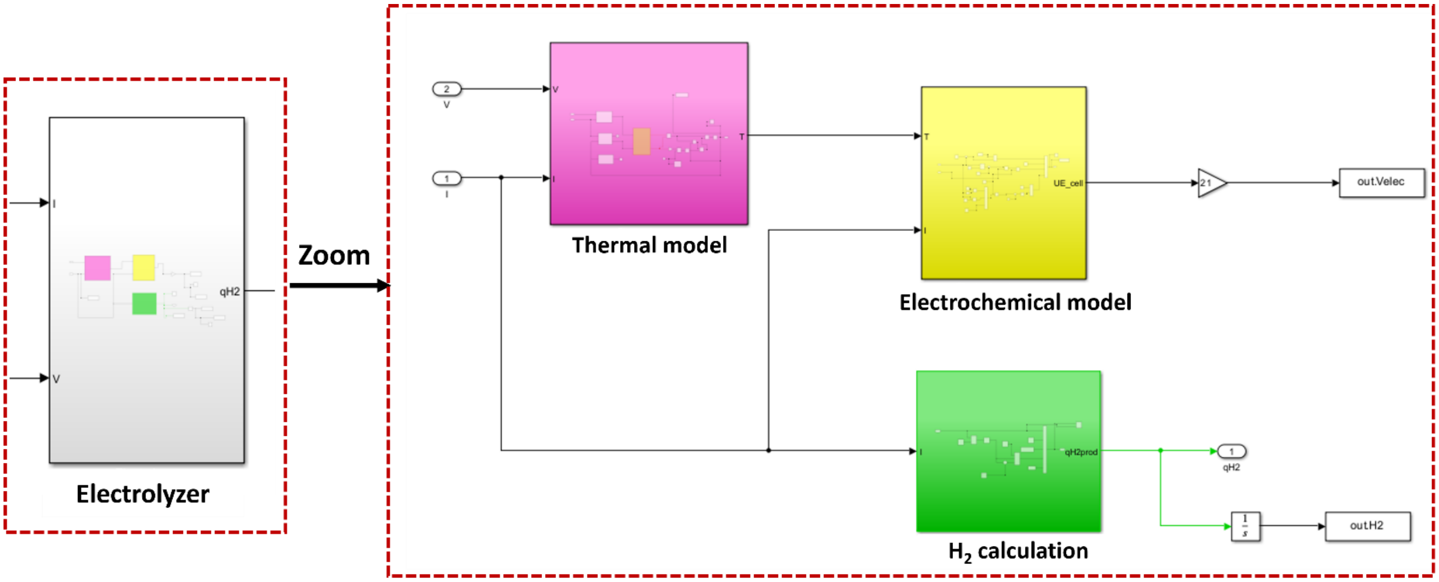

Figure 5. The MATLAB/Simulink sub-blocks of the Solar Panel model

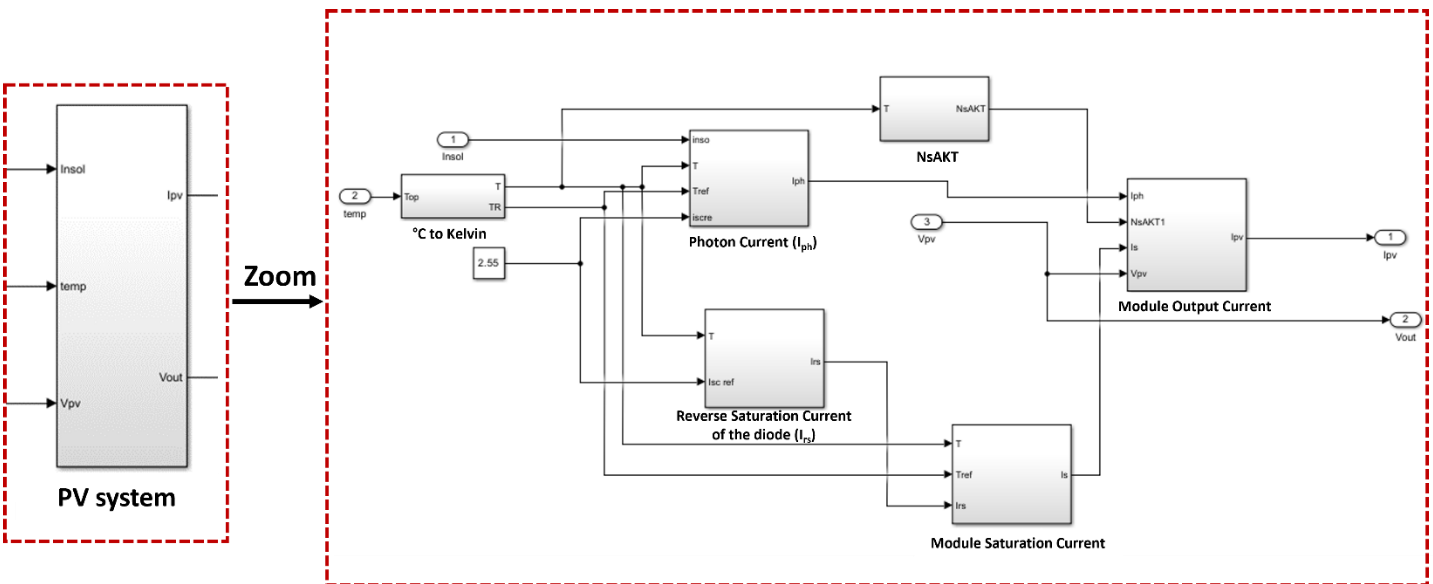

Figure 6. The MATLAB/Simulink sub-blocks of the electrolyzer

because increased solar irradiance leads to greater generation of electrical current in the photovoltaic cells. Conversely, at lower irradiation levels, such as 200 W/m^2, the module current is lower across the voltage range. This relationship is consistent with the basic behaviour of photovoltaic systems, where the amount of electricity generated is directly proportional to the intensity of incident sunlight.

In the other hand, the Figure 9 depicts the relationship between module power (P_{PV}) and module voltage (V_{PV}) under varying irradiation conditions. Similar to the module current graph, each curve represents a different irradiation level: 200 W/m^2, 600 W/m^2, and 1000 W/m^2. It is evident that module power exhibits a quadratic relationship with module voltage, as expected from the fundamental characteristics of photovoltaic systems. At higher irradiation levels, the module power curve is shifted upwards, indicating greater power output across the voltage range. Conversely, at lower irradiation levels, the module power curve is shifted downwards, reflecting reduced power output. This behaviour highlights the direct influence of solar irradiance on the power generation capabilities of photovoltaic modules, with higher irradiance levels resulting in increased power output and vice versa.

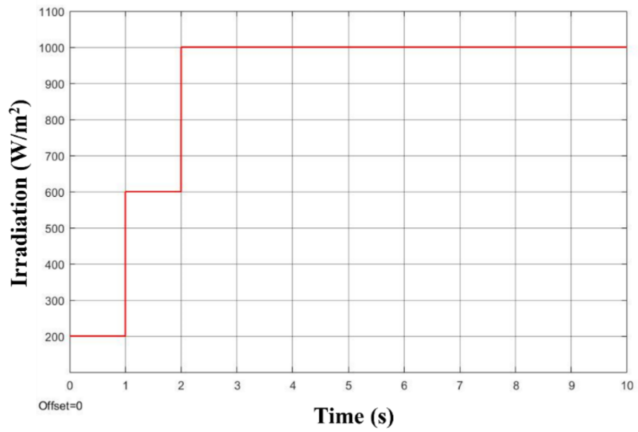

Figure 7. Input – Time varying irradiation

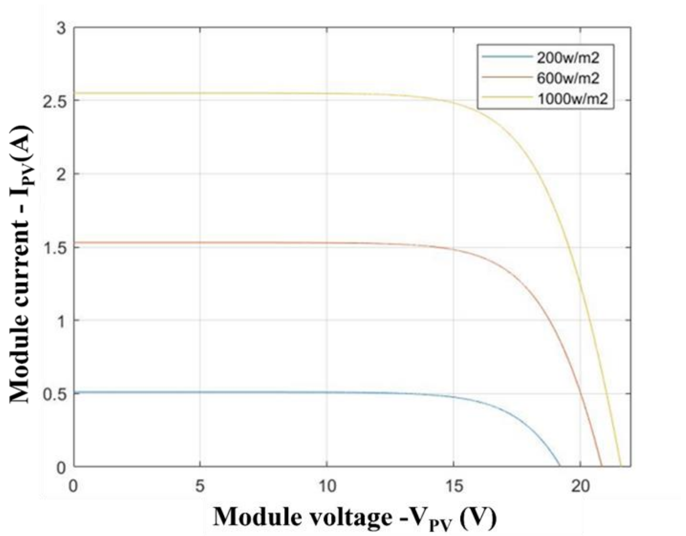

Figure 8. Module current – I-V characteristics with varying irradiation.

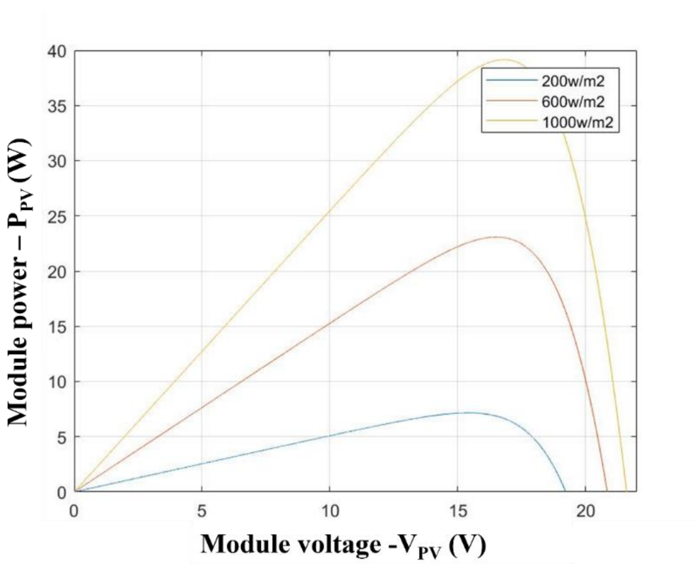

Figure 9. Module power – P-V characteristics with varying irradiation

- **PV (30 cells) - Electrolyzer**

The PV system with 30 cells connected in parallel ($N_p = 30$) was further investigated in conjunction with the electrolyzer. Applying the Eq. (4), using $N_p = 30$ giving us the I_{PV} and V_{PV} output for the PV as presented in Figure 10.

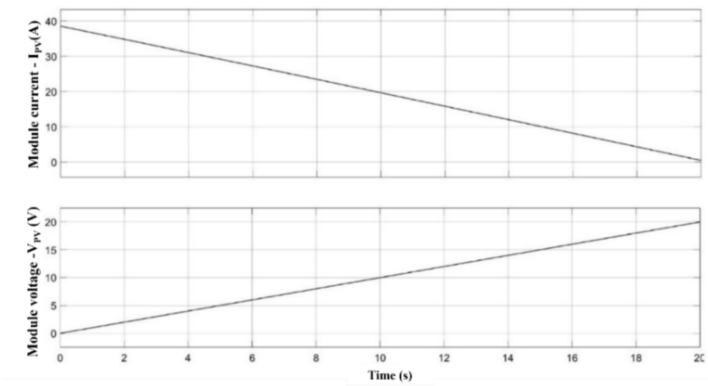

Figure 10. PV module current (I_{PV}) and voltage (V_{PV}) using 30 cells parallel.

The electric current generated from a power photovoltaic array in Figure 10 is used as an input signal changing in time with solar radiation. Based on this simulation results, it is observed that at the beginning of the simulation (0 s), the module current (I_{PV}) is 40 A, indicating a high initial current output from the PV system. At the same time, the module voltage (V_{PV}) is 0 V, suggesting that the voltage output is initially low. Over the course of the simulation from 0 to 20 s, the module current (I_{PV}) decreases gradually from 40 A to 0 A. This decrease in current indicates a reduction in the electrical output of the PV system over time. Concurrently, the module voltage (V_{PV}) increases steadily from 0 V to 20 V during the 20 s simulation period. This increase in voltage suggests that the voltage output of the PV system rises as the simulation progresses. These observations are consistent with the typical behaviour of a PV system. Initially, when there is sufficient sunlight, the PV system generates a high current but with a low voltage output. As time passes and the simulation progresses, the current output decreases while the voltage output increases, reflecting changes in the external conditions (e.g., solar irradiance, temperature) or the system's internal dynamics.

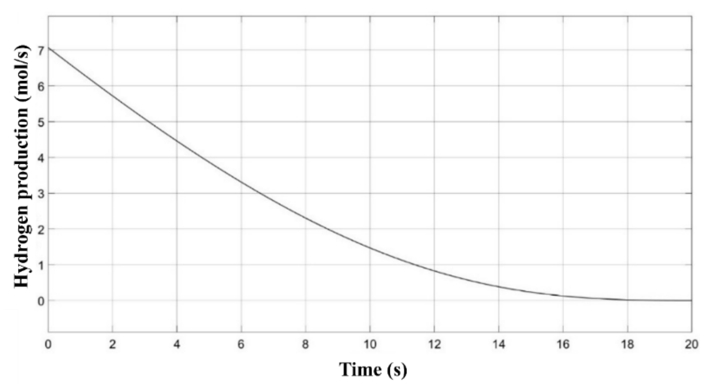

Figure 11. Production of hydrogen in moles per second

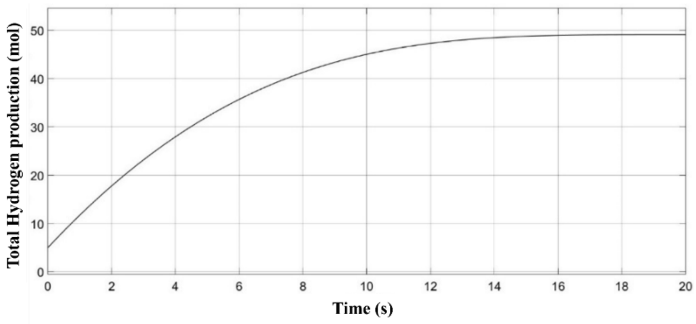

Figure 12. Total produced hydrogen in mol.

The results obtained during simulation of the hydrogen quantities are presented in Figure 11. Then the total produced hydrogen in depicted in Figure 12.

Figures 11 and 12 depict the hydrogen flow rates observed at various temperatures. Across the duration of the simulation, there is a noticeable decline in the rate of hydrogen production from an initial value of 7 mol/s to approximately 0 mol/s by the end of the 20 s. It can be attributed to various factors, including changes in operating conditions such as temperature variations or depletion of reactants over time. Additionally, it suggests a gradual decrease in the efficiency of the hydrogen generation process as the simulation progresses. While Figure 12 represents the cumulative amount of hydrogen produced over time in moles. Starting from an initial value of 5 mol at t = 0 s, the total produced hydrogen steadily increases throughout the simulation period, reaching a final value of approximately 50 mol at t = 20 s. This accumulation of hydrogen over time reflects the continuous operation of the hydrogen generation system and the progressive conversion of water into hydrogen gas. Despite the decrease in the rate of hydrogen production observed in Figure 11, the cumulative amount of hydrogen continues to rise due to the continuous operation of the system.

In addition, as the current increases, the hydrogen flow rate also increases, indicating a direct correlation between current supply and hydrogen production. The dissociation reaction responsible for breaking the bonds of water molecules is facilitated by the increasing current supply to the electrolyzer. Higher current densities lead to greater dissociation reactions, resulting in higher hydrogen flow rates.

4. Discussion

The study demonstrates the potential of harnessing solar energy for electrolysis, showcasing consistent hydrogen flow rates across diverse operational scenarios. This underscores the comparable performance of the integrated PV electrolysis system with prior research, as reported in the existing literature [18]. Through simulations, consistent hydrogen production rates are observed despite fluctuations in current supply and solar irradiance, aligning with observations from previous studies [19]. The comprehensive design model developed in the study serves as a springboard for future research avenues, such as maximizing hydrogen production efficiency and minimizing energy losses, as suggested in prior literature [20]. These endeavors aim to optimize the performance of PV-electrolyzer systems and unlock the full potential of solar-driven hydrogen production. The findings not only highlight the viability of solar-powered electrolysis but also provide a solid groundwork for further advancements in renewable energy technology. By focusing on refining system efficiency and reducing energy wastage, a contribution can be made to a more sustainable energy landscape [21 – 22].

5. Conclusions

In this paper, the production of hydrogen through water electrolysis is explored, utilizing an alkaline electrolyzer in conjunction with a photovoltaic (PV) system. Central to the study was the development and modeling of PV panel and alkaline electrolyzer models within the Simpower Systems block of MATLAB/Simulink, facilitating the simulation and analysis of the hydrogen production process. Through rigorous simulations, the amount of hydrogen generated by the integrated PV-electrolyzer system under various operating conditions was quantified. This empirical data provides valuable insights into the system's performance and efficiency, serving as a foundational step towards optimizing hydrogen production processes. Moving forward, the research will extend to exploring energy storage solutions aimed at mitigating the technical challenges associated with solar energy, wind power, and other intermittent generators. By addressing the intermittency issues inherent in renewable energy sources, the aim is to facilitate their seamless integration with utility grids. Energy storage technologies offer a promising avenue for enhancing grid stability, reducing reliance on fossil fuels, and fostering the widespread adoption of renewable energy. By continuing to investigate and develop innovative energy storage solutions, the path can be paved for a more sustainable and resilient energy future. Through collaborative efforts across academia, industry, and government sectors, the transition towards a greener and more sustainable energy landscape can be accelerated, driving positive environmental and socio-economic impacts globally.

Acknowledgment

This work was carried out at Altran Prototypes Automobiles (APA) as a part of the Intelligence & Innovation Powertrain (*IPWT*) project within the Capgemini Engineering Research and Innovation Department. The authors would like to thank the other members of the team, Chayma Mohsni, Mohand-Ouyahia Bousseksou, Adrien Soloy and Racha Bayzou for their valuable contributions to this work.

Conflict of Interest Statement

F.H and I.M. contributed equally. All authors have given approval to the final version of the manuscript. The authors declare that there is no conflict of interest in the study.

CRediT Author Statement

Fatima Haidar: Writing original draft- review & editing, Conceptualization, Supervision, Validation. **Imen Mrad:** Writing original draft; Data collection; Simulation, Validation. **Quang Truc Dam:** Writing original draft; Validation.

References

1. Aouali, F. Z., Becherif, M., Tabanjat, A., Emziane, M., Mohammedi, K., Krehi, S., & Khellaf, A. (2014). Modelling and Experimental Analysis of a PEM Electrolyser Powered by a Solar Photovoltaic Panel. Energy Procedia, 62, 714–722.

2. Hervello, M., Alfonsín, V., Sánchez, Á., Cancela, Á., & Rey, G. (2014). Simulation of a stand-alone renewable hydrogen system for residential supply. DYNA, 81(185), 116.
3. Kiaee, M., Cruden, A., Chladek, P., & Infield, D. (2015). Demonstration of the operation and performance of a pressurised alkaline electrolyser operating in the hydrogen fuelling station in Porsgrunn, Norway. Energy Conversion and Management, 94, 40–50.
4. Kamal, T., & Hassan, S. Z. (2016). Energy Management and Simulation of Photovoltaic/Hydrogen/Battery Hybrid Power System. Advances in Science, Technology and Engineering Systems Journal, 1(2), 11–18.
5. Awad, H., Abdalfatah, S., Hegazy, H., & Elkholy, E. E. (2019). Hybrid PV/FC System Design and Simulation. 2019 21st International Middle East Power Systems Conference (MEPCON), 1025–1030.
6. Zhou, T., & Francois, B. (2009). Modeling and control design of hydrogen production process for an active hydrogen/wind hybrid power system. International Journal of Hydrogen Energy, 34(1), 21–30.
7. Saeed, Eng. W., & Warkozek, Eng. G. (2015). Modeling and Analysis of Renewable PEM Fuel Cell System. Energy Procedia, 74, 87–101.
8. Awasthi, A., Scott, K., & Basu, S. (2011). Dynamic modeling and simulation of a proton exchange membrane electrolyzer for hydrogen production. International Journal of Hydrogen Energy, 36(22), 14779–14786.
9. Tijani, A. S., Yusup, N. A. B., & Rahim, A. H. A. (2014). Mathematical Modelling and Simulation Analysis of Advanced Alkaline Electrolyzer System for Hydrogen Production. Procedia Technology, 15, 798–806.
10. Lajnef, T., Abid, S., & Ammous, A. (2013). Modeling, Control, and Simulation of a Solar Hydrogen/Fuel Cell Hybrid Energy System for Grid-Connected Applications. Advances in Power Electronics, 1–9.
11. Ulleberg, O. (2003). Modeling of advanced alkaline electrolyzers: A system simulation approach. International Journal of Hydrogen Energy, 28(1), 21–33.
12. Cao, T.-F., Mu, Y.-T., Ding, J., Lin, H., He, Y.-L., & Tao, W.-Q. (2015). Modeling the temperature distribution and performance of a PEM fuel cell with thermal contact resistance. International Journal of Heat and Mass Transfer, 87, 544–556.
13. Megía, P. J., Vizcaíno, A. J., Calles, J. A., & Carrero, A. (2021). Hydrogen Production Technologies: From Fossil Fuels toward Renewable Sources. A Mini Review. Energy & Fuels, 35(20), 16403–16415.
14. Chowdhury, S., Chowdhury, S. P., Taylor, G. A., & Song, Y. H. (2008). Mathematical Modelling and Performance Evaluation of a Stand-Alone Polycrystalline PV Plant with MPPT Facility. 2008 IEEE Power and Energy Society General Meeting - Conversion and Delivery of Electrical Energy in the 21st Century, 1–7.
15. Pandiarajan, N., & Muthu, R. (2011). Mathematical modeling of photovoltaic module with Simulink. 2011 1st International Conference on Electrical Energy Systems, 258–263.
16. Jung, J.-H., & Ahmed, S. (2010). Model construction of single crystalline photovoltaic panels for real-time simulation. 2010 IEEE Energy Conversion Congress and Exposition, 342–349.
17. Bousseksou, O. (2024). Thermal modeling of solid hydrogen storage in a LaNi5 metal hydrid tank. Engineering Perspective, 1(1), 32–39.
18. Nasser, M., Megahed, T. F., Ookawara, S., & Hassan, H. (2022). A review of water electrolysis–based systems for hydrogen production using hybrid/solar/wind energy systems. Environmental Science and Pollution Research, 29(58), 86994–87018.
19. Fischer, M. (1986). Review of hydrogen production with photovoltaic electrolysis systems. International Journal of Hydrogen Energy, 11(8), 495–501.
20. Demirdelen, T., Ekinci, F., Mert, B. D., Karasu, İ., & Tümay, M. (2020). Green touch for hydrogen production via alkaline electrolysis: The semi-flexible PV panels mounted wind turbine design, production and performance analysis. International Journal of Hydrogen Energy, 45(18), 10680–10695.
21. Vinod, Kumar, R., & Singh, S. K. (2018). Solar photovoltaic modeling and simulation: As a renewable energy solution. Energy Reports, 4, 701–712.
22. Marocco, P., Gandiglio, M., & Santarelli, M. (2024). Optimal design of PV-based grid-connected hydrogen production systems. Journal of Cleaner Production, 434, 140007.